Marine Pollution Bulletin 207 (2024) 116914

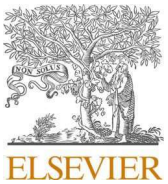

Contents lists available at ScienceDirect

Marine Pollution Bulletin

journal homepage: www.elsevier.com/locate/marpolbul

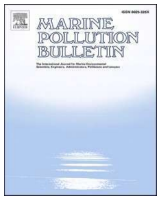

Efficient plastic detection in coastal areas with selected spectral bands

Ámbar Pérez-García [a,b,*], Tim H.M. van Emmerik [b], Aser Mata [c], Paolo F. Tasseron [b,d], José F. López [a]

[a] Institute for Applied Microelectronics, University of Las Palmas de Gran Canaria, Las Palmas de Gran Canaria, 35001, Spain
[b] Hydrology and Environmental Hydraulics Group, Wageningen University, Wageningen, 6708, BP, the Netherlands
[c] Digital Innovation and Marine Autonomy, Plymouth, Marine Laboratory (PML), Plymouth, PL1 3DH, United Kingdom
[d] Amsterdam Institute for Advanced Metropolitan Solutions, Amsterdam, 1018, JA, the Netherlands

ARTICLE INFO

Keywords:
Remote sensing
Macroplastic detection
Artificial intelligence
Band selection

ABSTRACT

Marine plastic pollution poses significant ecological, economic, and social challenges, necessitating innovative detection, management, and mitigation solutions. Spectral imaging and optical remote sensing have proven valuable tools in detecting and characterizing macroplastics in aquatic environments. Despite numerous studies focusing on bands of interest in the shortwave infrared spectrum, the high cost of sensors in this range makes it difficult to mass-produce them for long-term and large-scale applications. Therefore, we present the assessment and transfer of various machine learning models across four datasets to identify the key bands for detecting and classifying the most prevalent plastics in the marine environment within the visible and near-infrared (VNIR) range. Our study uses four different databases ranging from virgin plastics under laboratory conditions to weather plastics under field conditions. We used Sequential Feature Selection (SFS) and Random Forest (RF) models for the optimal band selection. The significance of homogeneous backgrounds for accurate detection is highlighted by a 97 % accuracy, and successful band transfers between datasets (87 %–91 %) suggest the feasibility of a sensor applicable across various scenarios. However, the model transfer requires further training for each specific dataset to achieve optimal accuracy. The results underscore the potential for broader application with continued refinement and expanded training datasets. Our findings provide valuable information for developing compelling and affordable detection sensors to address plastic pollution in coastal areas. This work paves the way towards enhancing the accuracy of marine litter detection and reduction globally, contributing to a sustainable future for our oceans.

1. Introduction

Marine litter, particularly plastic pollution, has become a pervasive problem affecting terrestrial and aquatic ecosystems globally, leading to significant ecological, economic, and health impacts. Single-use plastics and inadequate waste management practices have led to vast contamination of rivers and oceans Morales-Caselles et al. (2021), posing significant challenges to the environment Meijer et al. (2021). Plastic debris accumulation in marine environments threatens wildlife and habitats and challenges maritime industries and coastal communities Jambeck et al. (2015). Identifying polymer types is relevant because each plastic type has distinct impacts, sources, and transport behaviours, making its identification crucial for a comprehensive understanding Andrady (2011); Rochman et al. (2013). Monitoring plastic pollution is crucial for establishing a baseline understanding to track changes, identify hotspots, and assess the efficacy of implemented measures van Emmerik et al. (2023); Tasseron et al. (2024).

In situ monitoring of floating marine plastic debris, such as net surveys and visual observation, can be expensive, time-consuming, and requires expert supervision Armitage et al. (2022). Recent advances in remote sensing (RS) using multi- and hyperspectral imagery are promising for detecting macroplastics (≥0.5 cm) pollution from space Lebreton et al. (2018); Topouzelis et al. (2021); Schreyers et al. (2022). RS provides significant advantages over traditional methods by enabling efficient and continuous data acquisition and overcoming geographical and resource limitations Biermann et al. (2020). Additionally, uncrewed aerial vehicles (UAVs) have the potential for long-term plastic monitoring, offering advantages such as improved spatial resolution, quick response time, and lower operational costs Andriolo et al. (2023).

Numerous object detection and classification machine learning tools

* Corresponding author at: Institute for Applied Microelectronics, University of Las Palmas de Gran Canaria, Las Palmas de Gran Canaria, 35001, Spain.
E-mail address: ambar.perez@ulpgc.es (Á. Pérez-García).

https://doi.org/10.1016/j.marpolbul.2024.116914
Received 12 July 2024; Received in revised form 29 August 2024; Accepted 29 August 2024
Available online 7 September 2024

have been developed to monitor plastics in aquatic environments van Lieshout et al. (2020); Cortesi (2021); Rußwurm et al. (2023). Efforts have also been made to enhance detection from space using fusion Kremezi et al. (2022) and unmixing techniques Papageorgiou et al. (2022), and a benchmark dataset with Sentinel-2 images has been created to compare the performance of various artificial intelligence algorithms Kikaki et al. (2022). Nevertheless, there is a need for affordable and standardized plastic detection methods and equipment to address the challenges of monitoring plastic pollution on a global scale Martínez-Vicente et al. (2019); Cózar et al. (2024).

Current hyperspectral sensors are expensive and require considerable computational resources. Most macroplastic studies focus on the near-infrared (NIR) to shortwave infrared (SWIR) range, particularly around 1150 nm, where distinct absorption peaks facilitate plastics identification Garaba and Dierssen (2020). However, as detectors in the SWIR over 1000 nm are more expensive than in the visible and near-infrared (VNIR), between 400 and 1000 nm, implementing a multispectral sensor in the VNIR for plastic detection worldwide would lead to a significant reduction in costs Pérez-García et al. (2023). Several studies suggest that a high level of spectral detail is unnecessary for detecting and classifying other pollutants with gradually changing spectral signatures Legleiter et al. (2019, 2022); Pérez-García et al. (2024b). This indicates that sensors with broader bands could still provide reliable plastic classification. Therefore, we envision an affordable multispectral sensor with selected spectral bands for plastic detection.

We present an assessment of various machine learning models across different datasets to identify the key spectral bands for classifying the most prevalent marine plastics. By evaluating the transferability of these key bands across the datasets, we show that a sensor using these bands could identify plastics in various scenarios and conditions. Therefore, our study explores the feasibility of developing a VNIR multispectral sensor for detecting and identifying coastal macroplastics. This technology aims to enhance plastic recovery efforts in both field and spaceborne remote sensing, supporting the transition towards improved ocean health.

2. Materials and methods

In this paper, we applied a refined band selection methodology to different plastic datasets to select the optimal number of bands and to identify the bands of interest for the detection and classification of plastics. We used spectral information from three datasets covering various scenarios, from laboratory experiments without a background signal to sand and pebble beaches. Based on classification and feature selection methods, we identified bands of interest for plastic detection and evaluated the transferability across the datasets. Finally, we test its applicability by transferring the bands of interest to a fourth new dataset collected for the study.

2.1. Datasets

We focused on plastic polymers that are most common in coastal and marine environments Schwarz et al. (2019); Morales-Caselles et al. (2021); Barry et al. (2023), and which are present across all the datasets used in this study. These include high-density polyethylene (HDPE) for bottles, low-density polyethylene (LDPE) for bags, polypropylene (PP) for containers, and polystyrene (PS), which is represented in both its foamed (expanded polystyrene, EPS) and non-foamed forms. The four datasets contain items from the four plastic classes (HDPE, LDPE, PP, and PS) under different conditions.

We used hyperspectral imagery of virgin rectangular sheets from the HyperDrone (HD) project, where the sheets were placed on two different Scottish beaches: the sandy, seaweed-covered Tyninghame Beach (56.01° N, −2.59° W) in 2020 and the pebble-stone shore near Oban Airport (56.46° N, −5.40° W) in 2021. The measures were made with The Headwall Co-aligned VNIR and SWIR imager (NERC Field Spectroscopy Facility) Headwall Photonics (2020), which collects about 600 bands ranging from 450 to 2500 nm. The third dataset (WUR) is mainly composed of virgin plastic everyday items from domestic sources Tasseron et al. (2021a). The images were taken in the laboratory using Specim Fx10 and Fx17 cameras (Konica Minolta Company, Oulu, Finland) Specim Spectral Imaging (2019). Together, they range from 400 to 1700 nm, with about 300 bands. Fig. 1 presents an overview of the three datasets used to train the model. These datasets are available for further details; see Plymouth Marine Laboratory; Mata, A. (2023a) (HD20), Plymouth Marine Laboratory; Mata, A. (2023b) (HD21) and Tasseron et al. (2021b) (WUR).

We collected a new dataset comprising everyday plastics, with plastic bags, jars, bottles, and cups similar to those in the WUR dataset. This dataset serves as the testing ground for evaluating the model's applicability. The image was captured on a plain background with the Specim Fx10 and Fx17 cameras, following the WUR dataset procedure Tasseron et al. (2021a). Further information and the mean spectral signatures of this dataset are provided in Section 3.3.

2.2. Band selection methodology

The methodology determines the bands of interest based on a combination of classification and feature selection algorithms (Fig. 2) Pérez-García et al. (2024a).

Half of the data is used to train the classification models, of which 60 % belong to the training dataset, 30 % are for the test dataset, and 10 % for validation. We used Random Forest (RF) Ho (1995) and Support Vector Machine (SVM) Hearst et al. (1998) as classifiers, both with hyperparameter optimization. The feature selection algorithms are trained with the remaining half of the data and provided with the impurity-based feature importance of the classifiers to determine the best bands for classification. The feature selection algorithms used are

(a) HD20 (b) HD21

(c) WUR

Fig. 1. Datasets overview Plymouth Marine Laboratory; Mata, A. (2023a,b); Tasseron et al. (2021b).

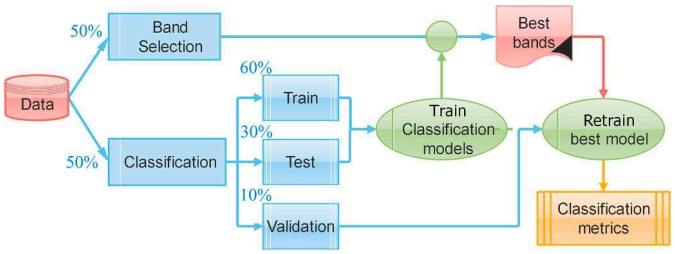

Fig. 2. Band selection methodology diagram Pérez-García et al. (2024a).

Sequential Feature Selector with forward selection (SFS) and Select From Model (SFM), both from the Python Scikit-Learn library Kramer (2016). SFS progressively includes or excludes features to optimize a classifier's performance, providing the optimized subset of features. SFM evaluates features based on their feature importance for the classifier Kramer (2016).

The optimal number of bands is determined using the elbow method Syakur et al. (2018), identifying the point on the accuracy curve where improvement slows, forming an "elbow." For the optimal number of bands, all classification metrics were calculated. Using only the best bands, the optimized classification models are re-trained. The validation dataset determines the classification metrics to assess performance. The overall accuracy (OAC) measures the ratio of correct predictions over the total number of samples Hossin and Sulaiman (2015). The F1 score is particularly useful with uneven class distribution, giving more importance to the accuracy of the smaller classes Boughorbel et al. (2017). The Kappa statistic (κ) measures inter-rater agreement for categorical items, correcting the bias that might occur due to chance agreement, especially with imbalanced datasets Cohen (1960).

Finally, we can evaluate the transferability of our results to different scenarios. This includes transferring bands of interest or pre-trained classification models. Transferring bands of interest involves using the identified wavelengths from one scenario to train a classifier in another scenario. The model transfer is challenging, as these models are tailored to specific scenario characteristics. If the spectral behaviour is sufficiently similar across scenarios, models can be effectively transferred, reducing the need for re-training the classifier and the computational time Pérez-García et al. (2024b).

Three measures of homogenization are applied to conduct a comparative study between the three datasets. First, the VNIR spectral range is selected, and the spectral ranges for which there is no data in all datasets are discarded. Therefore, the wavelengths of the study range from 490 to 850 nm. Second, the study only includes those elements of the datasets that match the target plastic types. From HD datasets: virgin EPS (PS class), agricultural PP, white HDPE net, and transparent LDPE, and from WUR: shampoo bottle and soap flask (HDPE), packaging bag (LDPE), bottle cap and food container (PP), and one-use white coffee stirrers (PS). The analysis includes backgrounds such as seaweed, rocks, and wet and dry sand. Third, to prevent misclassification caused by unbalanced classes, pixels from each dataset are randomly selected until each class contains 2700 samples, matching the number of pixels in the smallest class (PS in HD21).

3. Experiments

We designed three experiments in this study. Experiment 1 includes an individual dataset analysis, which offers insights into its complexity. Furthermore, optimizing the hyperparameters of the band selection model allows for determining the optimal number of bands needed for the multispectral sensor. Experiment 2 focuses on transferring the results and involves applying the findings obtained by training the model with one dataset to another. It is possible to transfer both the bands of interest and the pre-trained models, providing an understanding of the model adaptability. In experiment 3, the results from experiments 1 and 2 are applied to a real case study with a new dataset to quantify its performance.

3.1. Experiment 1: individual dataset analysis

Selecting the optimal number of bands poses one of the most challenging aspects of dataset analysis. Fig. 3 presents the OAC as a function of the number of bands used to train the model. The dataset achieving the highest level of accuracy is HD20 (97 %), whereas HD21 exhibits the lowest accuracy (93 %). The analysis indicates that SFS presents better accuracy than SFM, and its combination with RF further enhances performance. According to the elbow method Syakur et al. (2018), three bands are ideal. However, four bands are selected for the analysis, which is cost-effective and ensures better accuracy in transferring the research results Pérez-García et al. (2023).

The metrics performance is high across all datasets and for the different combinations of the model (0.690–0.959; see Table 1), validating the model adaptability. This substantiates that combining the SFS feature selection model with the RF classifier is the most effective. Therefore, the rest of the analysis concentrates on the results obtained using four bands and the SFS-RF method.

Fig. 3 also shows the confusion matrices for the three datasets, illustrating the performance of the optimized SFS-RF model with the four best bands for each dataset. Across all datasets, the classes with the poorest performance are HDPE and LDPE, between 9 % and 35 % of mutual misclassification. These results are consistent as both are polyethylene materials of different densities and are semi-transparent. The WUR dataset also identifies a 13 % of misclassification between HDPE and PP. Similar results are found in the HD datasets when including the background classes of the two datasets: seaweed, dry sand, wet sand, and rocks. Fig. 4 shows that all the backgrounds exceed 90 % accuracy, except for the rocks that achieve 89 % accuracy.

Combining SFS and RF models yields superior results for selecting key bands. The dataset with the highest performance with 4 bands is HD20, reaching 95.9 % OAC, 95.9 % F1-score, and 94.6 % κ. HD21

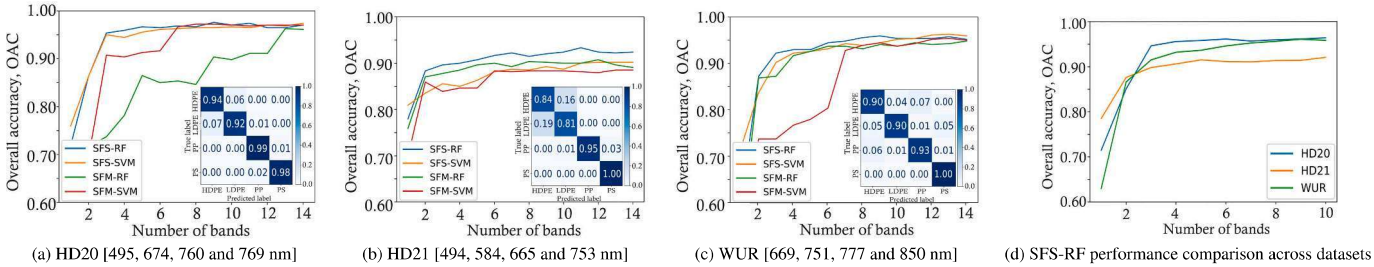

(a) HD20 [495, 674, 760 and 769 nm] (b) HD21 [494, 584, 665 and 753 nm] (c) WUR [669, 751, 777 and 850 nm] (d) SFS-RF performance comparison across datasets

Fig. 3. Overall accuracy of the model combination and confusion matrices for four bands per dataset.

Table 1
Metrics for all models with four bands in the VNIR.

		SFS			SFM		
		OAC	F1	κ	OAC	F1	κ
HD20	**RF**	**0.959**	**0.959**	**0.946**	0.781	0.781	0.708
	SVM	0.944	0.944	0.926	0.904	0.904	0.872
HD21	**RF**	**0.900**	**0.900**	**0.867**	0.885	0.885	0.847
	SVM	0.850	0.849	0.800	0.846	0.846	0.795
WUR	**RF**	**0.930**	**0.929**	**0.906**	0.917	0.917	0.889
	SVM	0.922	0.922	0.896	0.767	0.758	0.690

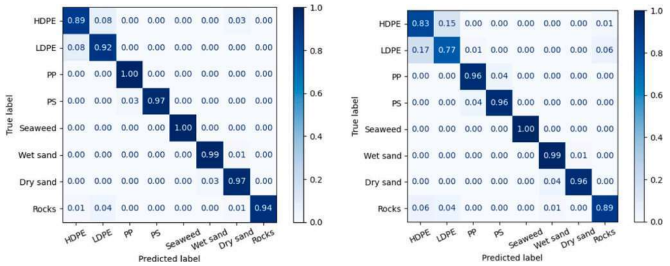

(a) HD20 (b) HD21

Fig. 4. HD dataset with backgrounds' confusion matrix (SFS-RF 4 bands).

exhibits the lowest performance, with 90.0 % OAC, 90.0 % F1-score, and 86.7 % κ. Moreover, distinguishing between the two densities of transparent polyethylene, HDPE and LDPE, and the rock background poses the most significant challenge in the individual dataset analysis. Section 3.2 discusses the transferability of results and trained models from one dataset to another.

3.2. Experiment 2: transfer learning

When applying a model across different scenarios, its transferability becomes crucial. The greater the model transferability, the broader its range of applications and the lower the computational costs by minimizing retraining efforts.

The initial step requires assessing the transferability of bands, i.e. whether the information resulting from training the model with one dataset can be extended to another without significant accuracy loss. We grouped the wavelengths into 25 nm widths to visualise the results. Fig. 5 shows the number of bands of interest in each designated spectral range. The greatest concentration of bands of interest where the three datasets coincide is in the NIR, between 750 and 800 nm, and in the red, around 650 nm. The two HD datasets also agree that the blue wavelengths between 475 and 500 nm provide relevant information. Finally, for HD21 yellow is of interest, concretely at 584 nm, and another band

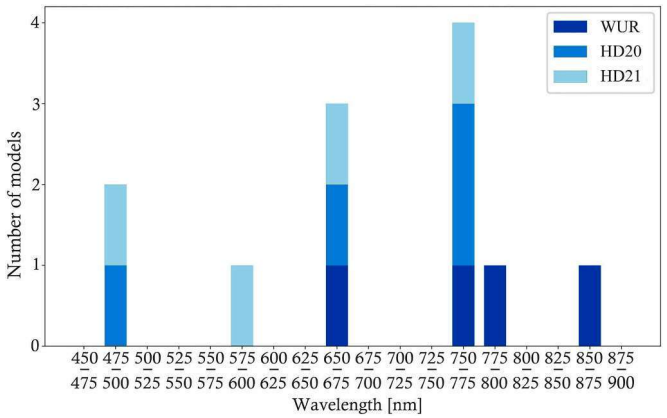

Fig. 5. First four bands of interest for each dataset.

appears in the NIR for WUR at 850 nm. Therefore, we can cover 9 out of the 12 bands of interest in the datasets using a multispectral camera with three bands in the spectral regions of coincidence—475-500 nm, 650–675 nm and 750–775 nm—, demonstrating band transferability.

In general, using the same dataset for both training and validation produces optimal results, as shown in Table 2 (by rows). The two HD datasets have the same plastics in different backgrounds (sand and pebbles). Training with 2021 and validating with 2020 gives better results than training and validating with 2021. The OAC suggests superior transfer occurs when training the model with the most heterogeneous dataset, WUR. This finding was unanticipated because both HD datasets use identical plastics.

The next step requires transferring the complete model and providing only the values of the validation dataset into the already trained classifier. When training with HD20 and transferring to HD21, the model achieves 80.8 % of OAC, while transferring from HD21 to HD20 results in 70.5 %. However, when transferring between HD and WUR datasets, the OAC varies between 25 % and 30 %, potentially attributable to the normalization of WUR spectra contrasted with the absence of normalization in HD spectra. Therefore, this phase is more complex to implement successfully and is more dependent on the dataset.

While band transfer proves effective, model transfer encounters certain limitations. Section 3.3 evaluates whether these limitations restrict its use to identical plastics or allow for broader application in a case study.

3.3. Experiment 3: case study

The final evaluation of the model's applicability involves providing it with entirely novel data, employing the dataset produced with everyday plastics. Fig. 6 (a) illustrates the everyday objects that constitute this dataset. As several objects lack the polymer identification code or recycling number standardized by ASTM (American Society for Testing and Materials), only the ones identified were used to validate the model: HDPE (no. 5, 8), LDPE (no. 13), PP (no. 11, 14), PS (no. 9, 15), with between 5500 and 7000 pixels per plastic type. Fig. 6 also shows the signatures of the objects used for the case study, with a distinct pattern for each plastic type.

Transferring the WUR SFS-RF model with four bands to the new dataset reaches 54.4 % accuracy, higher than that obtained for HD20 and HD21, 47 % and 41 %, respectively. Using the four bands of interest determined with the optimized SFS-RF model for any of the three datasets achieves an accuracy above 90 % in the new dataset. The confusion matrix in Fig. 6 (b) shows high performance, misclassifying only a few HDPE and PP pixels, which are the classes with the most similar spectral signatures and semitransparent in the VNIR range. Consequently, the transfer of results is considered successful.

4. Discussion

Our analysis provides a positive outlook for band transfer and classifying macroplastics in aquatic and coastal environments. Integrating SFS and RF models facilitates the optimal selection of bands of interest. The coincidence of the spectral regions of interest across datasets of different characteristics, coupled with the high accuracy (above 85 %) in terms of the number of bands employed and the transferability of the

Table 2
OAC for SFS-RF with four band transfer.

		Datasets providing the bands		
		HD20	**HD21**	**WUR**
Dataset validating the model	**HD20**	0.959	0.902	0.911
	HD21	0.889	0.900	0.891
	WUR	0.869	0.889	0.930

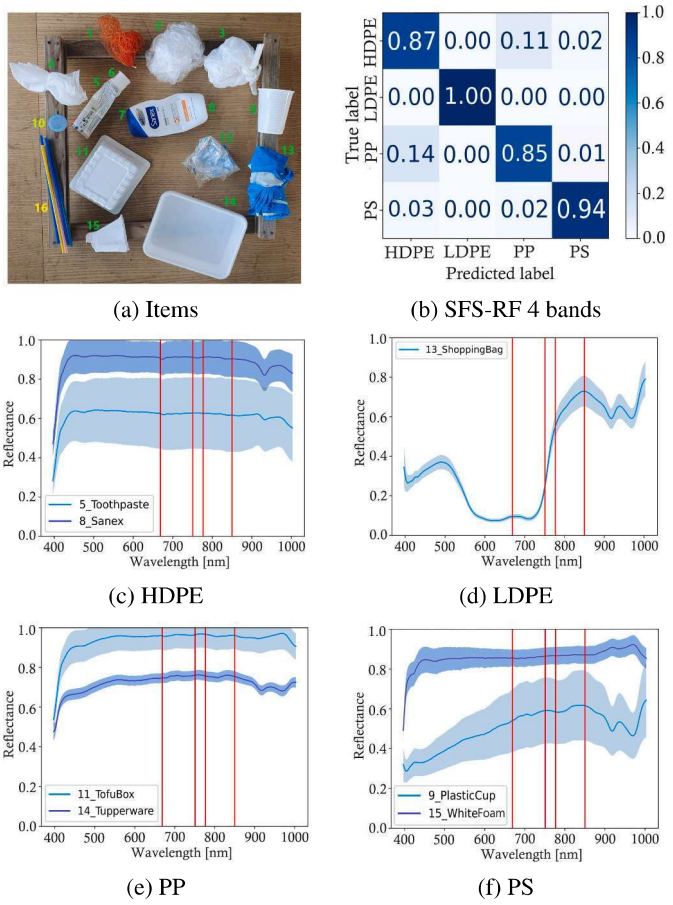

Fig. 6. Spectral analysis of the new dataset: objects, mean spectral signature with red lines indicating WUR best bands. (For interpretation of the references to colour in this figure legend, the reader is referred to the web version of this article.)

bands between datasets, enhances the sensor feasibility regarding efficiency.

The findings in Section 3.1 suggest that accuracy improves when the background is spectrally uniform, such as a sandy beach, where the spectral response is consistent across the area. This is particularly relevant due to the semi-transparent nature of some plastics. In contrast, a heterogeneous background, such as a pebble beach, introduces variability in light reflection both between and within individual pebbles, which introduces noise that hinders the identification of objects. Accordingly, HD21 exhibits the least favourable results in the study with 86.7 % κ. The HDPE and LDPE are usually semi-transparent, making them particularly susceptible to misclassification, reaching 35 % when both added in HD21.

The significance of a uniform background is evident in achieving better results, as also observed in Section 3.2. Training the model with HD20 and validating in HD21 outperforms the outcomes obtained when training and validating with the latter dataset. Training the model with heterogeneous objects helps to improve the transfer of the bands of interest, reducing the risk of the model overfitting. Despite the expectation of better band transfer between HD datasets due to the shared objects, the transfer from WUR to HD outperforms it, suggesting that incorporating heterogeneous objects is a valuable strategy for reducing overfitting.

The successful transfer of bands in the use case in Section 3.3, with an accuracy above 90 %, highlights the validity of the model and the conducted experiments. Since the bands of interest were determined by training the model on a different dataset, it is expected that they may not perfectly align with the spectral signatures of the new dataset. However, the robustness of the RF classifier allows it to effectively manage the classification of the limited number of objects in the study.

The main limitation lies in the model transfer. Although the accuracy exceeds 50 %, indicating promising performance, it also highlights that achieving high precision when transferring models between different datasets remains a challenge. Another limitation is that object colour can influence its spectral signature in the visible range, potentially leading to false positives or misclassification, particularly with darker-coloured plastics and transparent materials Zhu et al. (2020); Tasseron et al. (2022). Also, the reflectance of floating plastics is highly sensitive to plastic type, transparency, shape, and surface characteristics Martínez-Vicente et al. (2019); this effect is less pronounced for plastics on land. Our study focuses on light-coloured plastics found on land, where these issues are less significant and are not directly addressed. Future research could benefit from expanding the number of datasets and conducting more band transfers to datasets with varied backgrounds. This approach would help avoid overfitting the model to specific data, thereby improving the model transferability to other scenarios.

Within the context of previous research, several studies have explored the detection of macroplastics using similar RS techniques Topouzelis et al. (2021). In contrast to other SWIR-focused work Tasseron et al. (2022), our emphasis on the VNIR range explores the possibility of developing efficient, low-cost sensors. Several studies suggest that a high level of spectral detail is unnecessary for detecting and classifying other pollutants with gradually changing spectral signatures, indicating that sensors with broader bands could still provide reliable classification Legleiter et al. (2019, 2022). Our pipeline, which integrates various classification and feature selection models, enhances the methodology's effectiveness, surpassing other band selection techniques that need between 10 and 20 bands to achieve optimum accuracy Olyaei and Ebtehaj (2024).

To summarise, our findings contribute to a better understanding of plastics' spectral behaviour. The experiments' results advocate the feasibility of transferring bands of interest from one dataset to another for efficient macroplastic identification, highlighting the importance of training with heterogeneous datasets and uniform backgrounds.

5. Conclusion

This letter provides fundamental input for transferring classifiers across datasets to identify the key bands for detecting plastic pollution in aquatic environments. Integrating SFS and RF models optimizes band selection, enhancing sensor feasibility. Uniform backgrounds prove crucial for accurate detection, as seen in the individual findings, with successful differentiation of all polymers and backgrounds. Successful band transfers between datasets, with an accuracy of 90 %, highlight model validity. However, analysis of model transfer is limited, requiring classifier retraining in each dataset to achieve accuracy above 60 %. Consequently, while successful band transfers suggest the potential to develop a sensor capable of detecting plastics across various scenarios, the insufficient precision in model transfer indicates that the classifier must be trained for each scene. The study suggests expanding datasets to address limitations and improve model transferability. For optimal adaptability to various plastics, it is recommended to use a combination of bands from the three main datasets to cover different regions of the spectrum, with the sensor bands centred at 495 nm (blue), 665 nm (red), 777 nm (NIR) and 850 nm (NIR). In the near future, we will explore the effect of several multispectral sensor bandwidths on plastic classification and transferability to non-virgin plastics. In summary, these findings contribute to understanding the spectral behaviour of plastics and the effectiveness of band and model transfer, advocating for developing more targeted and adaptable remote sensing technologies for efficient plastic detection across diverse aquatic environments.

CRediT authorship contribution statement

Ámbar Pérez-García: Writing – review & editing, Writing – original draft, Visualization, Validation, Software, Methodology, Investigation, Formal analysis, Conceptualization. **Tim H.M. van Emmerik:** Writing – review & editing, Visualization, Supervision, Resources, Methodology, Conceptualization. **Aser Mata:** Writing – review & editing, Supervision, Resources, Conceptualization. **Paolo F. Tasseron:** Writing – review & editing, Data curation. **José F. López:** Writing – review & editing, Supervision, Resources, Project administration, Funding acquisition.

Declaration of generative AI and AI-assisted technologies in the writing process

While preparing this work, the authors used ChatGPT and Grammarly to improve the clarity and coherence of writing. The authors reviewed and edited the content as needed and took full responsibility for the publication's content.

Declaration of competing interest

The authors declare that they have no known competing financial interests or personal relationships that could have appeared to influence the work reported in this paper.

Data availability

The HD data collected are available at the CEDA Archive: HD20 is https://doi.org/10.5285/2485214239134768820ffb50fb5513bc and HD21 is https://doi.org/10.5285/e0f6a223220d463ea7a5d2a7520000cf. The WUR database is available online at https://doi.org/10.4121/14518278 (accessed on 4TU.ResearchData). The case study data will be made available on request.

Acknowledgements

This work was completed while Ámbar Pérez-García was beneficiary of a predoctoral grant given by the "Agencia Canaria de Investigacion, Innovacion y Sociedad de la Informacion (ACIISI)" of the "Consejería de Universidades, Ciencia e Innovación y Cultura", part-financed by the European Social Fund Plus (FSE+) "Programa Operativo Integrado de Canarias 2021-2027, Eje 3 Tema Prioritario 74 (85%)". We would also like to thank the OASIS-HARMONIE project, under contract PID2023-148285OB-C43 from "Proyectos de Generación de Conocimiento" 2023 and the PERSEO project, under contract CPP2021-008527, from "Programa de Colaboración Público-Privada" of "Gobierno de España", 2023-2025. We also extend our gratitude to the reviewers for their valuable insights.

References

Andrady, A.L., 2011. Microplastics in the marine environment. Mar. Pollut. Bull. 62, 1596–1605.

Andriolo, U., Topouzelis, K., van Emmerik, T.H., Papakonstantinou, A., Monteiro, J.G., Isobe, A., Hidaka, M., Kako, S., Kataoka, T., Gonçalves, G., 2023. Drones for litter monitoring on coasts and rivers: suitable flight altitude and image resolution. Mar. Pollut. Bull. 195, 115521.

Armitage, S., Awty-Carroll, K., Clewley, D., Martinez-Vicente, V., 2022. Detection and classification of floating plastic litter using a vessel-mounted video camera and deep learning. Remote Sens. (Basel) 14. https://doi.org/10.3390/rs14143425.

Barry, J., Rindorf, A., Gago, J., Silburn, B., McGoran, A., Russell, J., 2023. Top 10 marine litter items on the seafloor in european seas from 2012 to 2020. Sci. Total Environ. 902, 165997 https://doi.org/10.1016/j.scitotenv.2023.165997.

Biermann, L., Clewley, D., Martinez-Vicente, V., Topouzelis, K., 2020. Finding plastic patches in coastal waters using optical satellite data. Sci. Rep. 10, 5364.

Boughorbel, S., Jarray, F., El-Anbari, M., 2017. Optimal classifier for imbalanced data using Matthews correlation coefficient metric. PloS One 12, e0177678.

Cohen, J., 1960. A coefficient of agreement for nominal scales. Educ. Psychol. Meas. 20, 37–46.

Cortesi, I., 2021. Artificial intelligence applied to multispectral imagery for fluvial macroplastics detection, in: Proceedings of the joint international event 9th ARQUEOLÓGICA 2.0 & 3rd GEORES, pp. 495–497.

Cózar, A., Arias, M., Suaria, G., Viejo, J., Aliani, S., Koutroulis, A., Delaney, J., Bonnery, G., Macías, D., de Vries, R., et al., 2024. Proof of concept for a new sensor to monitor marine litter from space. Nat. Commun. 15, 4637.

van Emmerik, T.H., Kirschke, S., Schreyers, L.J., Nath, S., Schmidt, C., Wendt-Potthoff, K., 2023. Estimating plastic pollution in rivers through harmonized monitoring strategies. Mar. Pollut. Bull. 196, 115503.

Garaba, S.P., Dierssen, H.M., 2020. Hyperspectral ultraviolet to shortwave infrared characteristics of marine-harvested, washed-ashore and virgin plastics. Earth System Science Data 12, 77–86. https://doi.org/10.5194/essd-12-77-2020.

Hearst, M., Dumais, S., Osuna, E., Platt, J., Scholkopf, B., 1998. Support vector machines. IEEE Intelligent Systems and their Applications 13, 18–28. https://doi.org/10.1109/5254.708428.

Ho, T.K., 1995. Random decision forests, in: proceedings of 3rd international conference on document analysis and recognition, 1, 278–282. https://doi.org/10.1109/ICDAR.1995.598994.

Hossin, M., Sulaiman, M.N., 2015. A review on evaluation metrics for data classification evaluations. International journal of data mining & knowledge management process 5, 1.

Jambeck, J.R., Geyer, R., Wilcox, C., Siegler, T.R., Perryman, M., Andrady, A., Narayan, R., Law, K.L., 2015. Plastic waste inputs from land into the ocean. Science 347, 768–771.

Kikaki, K., Kakogeorgiou, I., Mikeli, P., Raitsos, D.E., Karantzalos, K., 2022. Marida: a benchmark for marine debris detection from sentinel-2 remote sensing data. PloS One 17, e0262247.

Kramer, O., 2016. Scikit-learn. Machine learning for evolution strategies 45–53.

Kremezi, M., Kristollari, V., Karathanassi, V., Topouzelis, K., Kolokoussis, P., Taggio, N., Aiello, A., Ceriola, G., Barbone, E., Corradi, P., 2022. Increasing the sentinel-2 potential for marine plastic litter monitoring through image fusion techniques. Mar. Pollut. Bull. 182, 113974.

Lebreton, L., Slat, B., Ferrari, F., Sainte-Rose, B., Aitken, J., Marthouse, R., Hajbane, S., Cunsolo, S., Schwarz, A., Levivier, A., et al., 2018. Evidence that the great pacific garbage patch is rapidly accumulating plastic. Sci. Rep. 8, 1–15.

Legleiter, C.J., Manley, P.V., Erwin, S.O., Bulliner, E.A., 2019. An experimental evaluation of the feasibility of inferring concentrations of a visible tracer dye from remotely sensed data in turbid rivers. Remote Sens. (Basel) 12, 57.

Legleiter, C.J., Sansom, B.J., Jacobson, R.B., 2022. Remote sensing of visible dye concentrations during a tracer experiment on a large, turbid river. Water Resour. Res. 58, e2021WR031396.

van Lieshout, C., van Oeveren, K., van Emmerik, T., Postma, E., 2020. Automated river plastic monitoring using deep learning and cameras. Earth and space science 7, e2019EA000960.

Martínez-Vicente, V., Clark, J.R., Corradi, P., Aliani, S., Arias, M., Bochow, M., Bonnery, G., Cole, M., Cózar, A., Donnelly, R., Echevarría, F., Galgani, F., Garaba, S. P., Goddijn-Murphy, L., Lebreton, L., Leslie, H.A., Lindeque, P.K., Maximenko, N., Martin-Lauzer, F.R., Moller, D., Murphy, P., Palombi, L., Raimondi, V., Reisser, J., Romero, L., Simis, S.G., Sterckx, S., Thompson, R.C., Topouzelis, K.N., van Sebille, E., Veiga, J.M., Vethaak, A.D., 2019. Measuring marine plastic debris from space: initial assessment of observation requirements. Remote sensing 11. https://www.mdpi.com/2072-4292/11/20/2443. https://doi.org/10.3390/rs11202443.

Meijer, L.J., Van Emmerik, T., Van Der Ent, R., Schmidt, C., Lebreton, L., 2021. More than 1000 rivers account for 80% of global riverine plastic emissions into the ocean. Science. Advances 7, eaaz5803.

Morales-Caselles, C., Viejo, J., Martí, E., González-Fernández, D., Pragnell-Raasch, H., González-Gordillo, J.I., Montero, E., Arroyo, G.M., Hanke, G., Salvo, V.S., et al., 2021. An inshore–offshore sorting system revealed from global classification of ocean litter. Nature Sustainability 4, 484–493.

Olyaei, M., Ebtehaj, A., 2024. Uncovering plastic litter spectral signatures: a comparative study of hyperspectral band selection algorithms. Remote Sens. (Basel) 16. https://doi.org/10.3390/rs16010172.

Papageorgiou, D., Topouzelis, K., Suaria, G., Aliani, S., Corradi, P., 2022. Sentinel-2 detection of floating marine litter targets with partial spectral unmixing and spectral comparison with other floating materials (plastic litter project 2021). Remote Sens. (Basel) 14, 5997.

Pérez-García, Á., Rodríguez-Molina, A., Hernández, E., Vera, L., López, J.F., 2023. Development of low-cost multi-spectral cameras for precision agriculture. IGARSS 2023–2023 IEEE International Geoscience and Remote Sensing Symposium 3466–3469. https://doi.org/10.1109/IGARSS52108.2023.10282072.

Pérez-García, Á., Lorenzo, A.M., López, J., 2024a. Spectral band selection methodology for future sensor development. 2024 47th MIPRO ICT and electronics convention (MIPRO) 152–156. https://doi.org/10.1109/MIPRO60963.2024.10569699.

Pérez-García, Á., Martín Lorenzo, A., Hernández, E., Rodríguez-Molina, A., van Emmerik, T.H.M., López, J.F., 2024b. Developing a generalizable spectral classifier for rhodamine detection in aquatic environments. Remote Sens. (Basel) 16, 1–18. https://doi.org/10.3390/rs16163090.

Headwall Photonics, 2020. Spectral imaging instruments. https://www.headwallphotonics.com. [online; accessed 22-Jun-2020].

Plymouth Marine Laboratory, Mata, A., 2023a. Hyperdrone flight 20200929 - hyperspectral in situ radiometry and hyperspectral imagery at different altitudes for plastics detection. NERC EDS Centre for Environmental Data Analysis. https://doi.org/10.5285/2485214239134768820ffb50fb5513bc.

Plymouth Marine Laboratory, Mata, A., 2023b. Hyperdrone flight 20210722 - hyperspectral in situ radiometry and hyperspectral imagery at different altitudes for

plastics detection. NERC EDS Centre for Environmental Data Analysis. https://doi.org/10.5285/e0f6a223220d463ea7a5d2a7520000cf.
Rochman, C.M., Hoh, E., Hentschel, B.T., Kaye, S., 2013. Long-term field measurement of sorption of organic contaminants to five types of plastic pellets: implications for plastic marine debris. Environ. Sci. Technol. 47, 1646–1654.
Rußwurm, M., Venkatesa, S.J., Tuia, D., 2023. Large-scale detection of marine debris in coastal areas with sentinel-2. iScience.
Schreyers, L., van Emmerik, T., Biermann, L., van der Ploeg, M., 2022. Direct and indirect river plastic detection from space. IGARSS 2022–2022 IEEE International Geoscience and Remote Sensing Symposium 5539–5542. https://doi.org/10.1109/IGARSS46834.2022.9883379.
Schwarz, A., Ligthart, T., Boukris, E., Van Harmelen, T., 2019. Sources, transport, and accumulation of different types of plastic litter in aquatic environments: a review study. Mar. Pollut. Bull. 143, 92–100.
Specim Spectral Imaging, 2019. FX Series hyperspectral cameras. http://www.specim.fi/fx/. [Online; accessed 06-Oct-2019].
Syakur, M., Khotimah, B., Rochman, E., Satoto, B.D., 2018. Integration k-means clustering method and elbow method for identification of the best customer profile cluster. IOP conference series: materials science and engineering, IOP publishing 336, 012017.
Tasseron, P., van Emmerik, T., Peller, J., Schreyers, L., Biermann, L., 2021a. Advancing floating macroplastic detection from space using experimental hyperspectral imagery. Remote Sens. (Basel) 13. https://doi.org/10.3390/rs13122335.
Tasseron, P., van Emmerik, T., Schreyers, L., Biermann, L., Peller, J., 2021b. Hyperspectral plastics dataset supplementary to the paper 'advancing floating plastic detection from space using hyperspectral imagery'. 4TU.ResearchData. https://doi.org/10.4121/14518278.V3.
Tasseron, P.F., Schreyers, L., Peller, J., Biermann, L., van Emmerik, T., 2022. Toward robust river plastic detection: combining lab and field-based hyperspectral imagery. Earth and space. Science 9, e2022EA002518.
Tasseron, P.F., van Emmerik, T.H., Vriend, P., Hauk, R., Alberti, F., Mellink, Y., van der Ploeg, M., 2024. Defining plastic pollution hotspots. Sci. Total Environ. 934, 173294 https://doi.org/10.1016/j.scitotenv.2024.173294.
Topouzelis, K., Papageorgiou, D., Suaria, G., Aliani, S., 2021. Floating marine litter detection algorithms and techniques using optical remote sensing data: a review. Mar. Pollut. Bull. 170, 112675 https://doi.org/10.1016/j.marpolbul.2021.112675.
Zhu, C., Kanaya, Y., Nakajima, R., Tsuchiya, M., Nomaki, H., Kitahashi, T., Fujikura, K., 2020. Characterization of microplastics on filter substrates based on hyperspectral imaging: laboratory assessments. Environ. Pollut. 263, 114296 https://doi.org/10.1016/j.envpol.2020.114296.